Biophysical Journal
Article

Biophysical Society

Omecamtiv Mecarbil Abolishes Length-Mediated Increase in Guinea Pig Cardiac Myofiber Ca^{2+} Sensitivity

Sampath K. Gollapudi,[1] Sherif M. Reda,[1] and Murali Chandra[1,*]
[1]Department of Integrative Physiology and Neuroscience (IPN), Washington State University, Pullman, Washington

ABSTRACT Omecamtiv mecarbil (OM) is a pharmacological agent that augments cardiac contractile function by enhancing myofilament Ca^{2+} sensitivity. Given that interventions that increase myofilament Ca^{2+} sensitivity have the potential to alter length-dependent activation (LDA) of cardiac myofilaments, we tested the influence of OM on this fundamental property of the heart. This is significant not only because LDA is prominent in cardiac muscle but also because it contributes to the Frank-Starling law, a mechanism by which the heart increases stroke volume in response to an increase in venous return. We measured steady-state and dynamic contractile indices in detergent-skinned guinea pig (*Cavia porcellus*) cardiac muscle fibers in the absence and presence of 0.3 and 3.0 μM OM at two different sarcomere lengths (SLs), short SL (1.9 μm) and long SL (2.3 μm). Myofilament Ca^{2+} sensitivity, as measured by pCa_{50} ($-$log of $[Ca^{2+}]_{free}$ concentration required for half-maximal activation), increased significantly at both short and long SLs in OM-treated fibers when compared to untreated fibers; however, the magnitude of increase in pCa_{50} was twofold greater at short SL than at long SL. A consequence of this greater increase in pCa_{50} at short SL was that pCa_{50} did not increase any further at long SL, suggesting that OM abolished the SL dependency of pCa_{50}. Furthermore, the SL dependency of rate constants of cross-bridge distortion dynamics (c) and force redevelopment (k_{tr}) was abolished in 0.3-μM-OM-treated fibers. The negative impact of OM on the SL dependency of pCa_{50}, c, and k_{tr} was also observed in 3.0-μM-OM-treated fibers, indicating that cooperative mechanisms linked to LDA were altered by the OM-mediated effects on cardiac myofilaments.

INTRODUCTION

Omecamtiv mecarbil (OM) is a cardiac-specific myosin activator that has been shown to improve cardiac function in both animal models and humans. At the whole-heart level, OM increases systolic function by increasing stroke volume and ejection fraction (1–4). The basis for OM-mediated enhancement of cardiac contractile function is highlighted by recent studies (5–8) demonstrating that OM increases cardiac myofilament Ca^{2+} sensitivity and tension. A recent study (5) also suggests that OM-mediated effects augment cross-bridge (XB)-based cooperative mechanisms such that cardiac thin filaments are activated, leading to an increase in myofilament Ca^{2+} sensitivity.

XB-mediated cooperative activation of thin filaments is also implicated in other fundamental aspects of cardiac muscle regulation. One such aspect is length-dependent activation (LDA), whereby a given increase in sarcomere length (SL) increases myofilament Ca^{2+} sensitivity to a greater extent in cardiac muscle compared to skeletal muscle (9–11). This enhanced dependency of myofilament Ca^{2+} sensitivity on SL in cardiac muscle relies on regulatory components of the cooperative system that respond steeply to feedback effects of strong XBs on thin filaments (9,12–15). At the whole-heart level, LDA may contribute to the Frank-Starling (FS) law (16–19), a mechanism by which the heart increases its stroke volume in response to an increase in venous return. With regard to cooperative activation of cardiac thin filaments, a consistent observation made in the last two decades of research is that interventions that alter XB-based cooperative mechanisms or modifications that enhance thin-filament Ca^{2+} sensitivity affect LDA (12,17,20). For example, NEM-S1 (a strong XB analog) significantly increases myofilament Ca^{2+} sensitivity at short SL by elevating cooperative recruitment of strong XBs such that an increase in SL leads to no further increase in myofilament Ca^{2+} sensitivity (12); in other words, NEM-S1 abolishes LDA. Likewise, expression of slow skeletal troponin I in cardiac muscle enhances myofilament Ca^{2+}

Submitted May 12, 2017, and accepted for publication July 5, 2017.
*Correspondence: murali@vetmed.wsu.edu
Editor: David Warshaw.
http://dx.doi.org/10.1016/j.bpj.2017.07.002

sensitivity but attenuates LDA (17) and R92L mutation in cardiac troponin T enhances myofilament Ca^{2+} sensitivity but abolishes LDA (20) in cardiac muscle fibers. Because OM also augments strong XB-based cooperative activation of thin filaments and myofilament Ca^{2+} sensitivity, the observations made above highlight the need to assess the OM-mediated effect on LDA. Whether or not the OM-mediated effects on cardiac myofilament alter LDA in cardiac muscle fibers remains unknown.

The physiological significance of understanding the effect of OM on LDA in cardiac muscle is highlighted by observations that LDA is impaired in patients with heart failure (21–23). There is also experimental evidence to suggest that attenuation of LDA at the myofilament level may translate as an impaired FS mechanism in the intact heart (16–19). To test the hypothesis that OM alters cardiac myofilament length-sensing mechanisms to modulate LDA, we characterized steady-state and dynamic contractile features in cardiac muscle fibers from *Cavia porcellus* (guinea pigs) in the absence and presence of 0.3 and 3.0 μM OM at short (1.9 μm) and long SLs (2.3 μm). Regardless of the OM concentration, steady-state contractile measurements demonstrated that myofilament Ca^{2+} sensitivity increased to a greater extent at short SL than at long SL; consequently, OM abolished the SL-dependent increase in myofilament Ca^{2+} sensitivity. Moreover, the SL dependency of XB turnover rate and XB detachment kinetics was abolished, suggesting that cooperative mechanisms associated with LDA were altered by the OM-mediated effects on cardiac myofilaments.

MATERIALS AND METHODS

Animal protocols

Six- to eight-month-old male Dunkin-Hartley guinea pigs (Charles River, Burlington, MA) were used in this study. All animals were housed in environmentally controlled rooms (accredited by the American Association for Laboratory Animal Care) under 12 h light and dark cycles and received proper care and treatment in accordance with the pre-approved protocols of the Washington State University Institutional Animal Care and Use Committee. The procedures for euthanizing guinea pigs conform to the recommendations of the American Veterinary Medical Association as outlined in the Guidelines for the Euthanasia of Animals.

Measurements of pCa-tension relationship

Left ventricular papillary muscle fibers from guinea pigs were prepared and detergent-skinned, as described in the Supporting Material. Muscle fibers were attached between a motor arm (322C; Aurora Scientific, Ontario, Canada) and a force transducer (AE 801; Sensor One Technologies, Sausalito, CA) using T-shaped aluminum clips. The resting SL of muscle fibers was adjusted to either 1.9 or 2.3 μm and steady-state tension measurements were made in various test solutions with pCa ($-\log$ of $[Ca^{2+}]_{free}$) ranging from 9.0 to 4.3. The compositions of pCa solutions are listed in the Supporting Material. The pH and ionic strength of pCa solutions were adjusted to 7.0 and 180 mM, respectively. All measurements were made at 20°C.

Preparation of OM solution

OM (CK-1827452) was acquired from Selleckchem (Houston, TX) and an initial 15 mM stock was prepared in dimethylsulfoxide (DMSO) as per the manufacturer's instructions. Appropriate volumes of concentrated OM stock solutions were added to various pCa solutions to achieve final concentrations ranging from 0.1 to 10 μM; the final concentration of DMSO was 0.5%. To make comparisons relevant, we also adjusted the final concentration of DMSO in pCa solutions used for control (untreated) fibers to 0.5%. During the experiment, each fiber was incubated in DMSO- or OM-containing solution for 10 min before making contractile measurements.

Dynamic muscle fiber stiffness

A series of various amplitude stretch/release perturbations ($\pm$0.5, $\pm$1.0, $\pm$1.5, and $\pm$2.0% of the initial muscle length (ML)) was applied on muscle fibers and the corresponding force responses were recorded (24). Representative traces of a 2% step-like increase in ML and the corresponding force response elicited by an untreated muscle fiber are shown in Fig. 1, *A* and *B*, respectively. A nonlinear recruitment-distortion (NLRD) model was fit to force responses (24) to estimate the following four model parameters: the magnitude of the instantaneous muscle fiber stiffness caused by a sudden change in ML (E_D); the rate at which the strain within bound XBs dissipates to a steady-state level (c); the rate at which new XBs are recruited into the force-bearing state due to a change in ML (b); and the magnitude of increase in the muscle fiber stiffness due to ML-mediated recruitment of additional force-bearing XBs (E_R). Details on the characteristic features of force responses to step-like length perturbations and the physiological significance of model parameters are included in the Supporting Material.

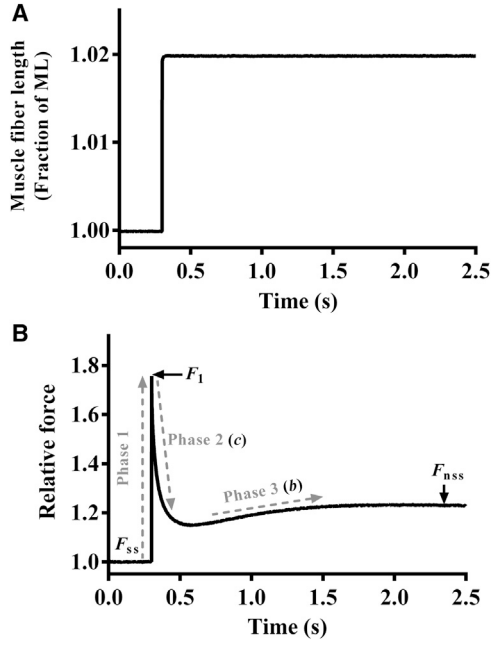

FIGURE 1 Force response to a sudden 2% stretch. (*A*) A representative 2% increase in ML imposed on a control (untreated) guinea pig cardiac muscle fiber at maximal Ca^{2+} activation (pCa 4.3). (*B*) The corresponding force responses normalized to the isometric steady-state force (F_{ss}) before ML change. Different phases (*dashed lines*) from which respective parameters were estimated are highlighted. F_1, the instantaneous increase in force due to sudden increase in ML (*phase 1*); c, the rate at which the sudden ML-induced strain within force-bearing XBs dissipates to a minimal force point (*phase 2*); b, the rate of delayed force rise after an increase in ML (*phase 3*); F_{nss}, the new steady-state force corresponding to an increase in ML.

Rate constant of tension redevelopment, k_{tr}

k_{tr} was estimated using force response in maximally activated muscle fibers in response to a large slack/restretch perturbation, as described in the Supporting Material.

Statistical analysis

Our experimental model involved two factors, treatment (untreated and OM-treated) and SL (1.9 and 2.3 μm). Therefore, we used two-way analysis of variance (ANOVA) to analyze the data. A significant treatment-SL interaction effect suggested that the effect of OM on a given contractile parameter varied significantly with SL. When the interaction effect was not significant, we assessed the main effects of both OM and SL. To probe the underlying cause for a significant interaction effect or a main effect, we performed multiple post hoc *t*-tests using Fisher's least-squares difference method. The criterion for statistical significance was set to $p < 0.05$. Data were presented as the mean ± SE.

RESULTS

Phosphorylation status of sarcomeric proteins in untreated and OM-treated fibers

To determine the phosphorylation status of sarcomeric proteins in untreated and OM-treated fibers, solubilized protein samples from untreated and OM-treated fibers were subjected to Pro-Q phospho-analysis, as described in the Supporting Material. The representative gel shown in Fig. S1 demonstrates that the phosphorylation levels of various sarcomeric proteins are similar in untreated and OM-treated fibers; this finding is in agreement with another recent study of OM (5).

Dose response of OM

We generated a dose-response curve for OM by measuring tension of muscle fibers exposed to various OM concentrations ranging from 0.1 to 10 μM at pCa 6.0. As illustrated in Fig. 2, tension increased progressively with increasing OM concentration, reaching a maximum value at 3 μM. The OM concentration required to attain a half-maximal effect (EC_{50}) in guinea pig was 0.36 μM, which is comparable to the EC_{50} of 0.31 μM reported in a previous study in mice (8). Our choice of low (0.3 μM) and high (3.0 μM) OM concentrations in this study spans the range of doses used in clinical trials (3).

Effect of OM on maximal tension and E_D

Two-way ANOVA of maximal tension (pCa 4.3) did not show a significant interaction effect ($p = 0.30$), but it showed significant main effects of both OM ($p < 0.05$) and SL ($p < 0.001$). To probe the underlying cause of significant effects of OM and SL on maximal tension, we performed post hoc *t*-tests. OM (0.3 μM) significantly increased maximal tension by 13% ($p < 0.05$; Fig. 3 *A*) at short SL, but it showed no significant effect ($p = 0.85$; Fig. 3 *A*) at long SL. Our observation at long SL (2.3 μm) is consistent with another study conducted at an SL of 2.24 μm (7). As for the main effect of SL on

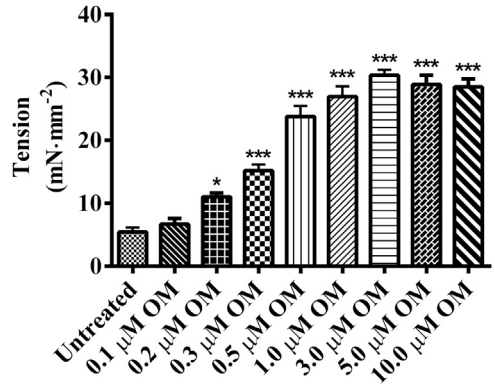

FIGURE 2 Dose response of OM. Steady-state tensions in muscle fibers were measured in pCa 6.0 solution, with OM concentration ranging from 0.1 to 10 μM. Tension increased with increasing OM concentration up to 3.0 μM and saturated thereafter. Asterisks indicate a significant difference from untreated fibers (*$p < 0.05$, ***$p < 0.001$; NS, not significant). A separate set of four fibers was measured at each concentration. Data are expressed as the mean ± SE.

Ca^{2+}-activated maximal tension, increasing the SL from 1.9 to 2.3 μm significantly increased maximal tension by 55% ($p < 0.001$; Fig. 3 *A*) in untreated fibers and by 41% ($p < 0.001$; Fig. 3 *A*) in 0.3-μM-OM-treated fibers. Fibers treated with 3.0 μM OM (Table S1) also substantiated our observations on maximal tension in 0.3-μM-OM-treated fibers.

We compared estimates of E_D (pCa 4.3) among groups to validate our observations on maximal tension. E_D was estimated from the instantaneous increase in force (F_1; Fig. 1 *B*) in response to a sudden increase in ML (Fig. 1 *A*), as described in the Supporting Material. We have previously shown that E_D is correlated with maximal tension and that it is an approximation of the number of force-bearing XBs (24–27). Two-way ANOVA of E_D did not show a significant interaction effect ($p = 0.62$), but it confirmed significant main effects of both OM ($p < 0.05$) and SL ($p < 0.01$). The 0.3 μM OM significantly increased E_D by 19% ($p < 0.01$; Fig. 3 *B*) at short SL but it did not show a significant effect ($p = 0.17$; Fig. 3 *B*) at long SL. An increase in SL significantly increased E_D by 20% ($p < 0.01$; Fig. 3 *B*) in untreated fibers and by 14% ($p < 0.05$; Fig. 3 *B*) in 0.3-μM-OM-treated fibers. Our observations on E_D were similar in both 0.3- and 3.0-μM-OM-treated fibers (Table S1).

Effect of OM on the pCa-tension relationship

pCa-tension plots showed a greater leftward shift in the pCa-tension relationship of 0.3-μM-OM-treated fibers at short (Fig. 4 *A*) than at long SL (Fig. 4 *B*). This suggested that OM induced a greater increase in myofilament Ca^{2+} sensitivity at short than at long SL. Fig. 4, *A* and *B*, also indicated a decrease in the steepness of the pCa-tension relationship in 0.3-μM-OM-treated fibers, suggesting that OM attenuated myofilament cooperativity. To quantify the magnitude of the OM-mediated effect on the pCa-tension relationship,

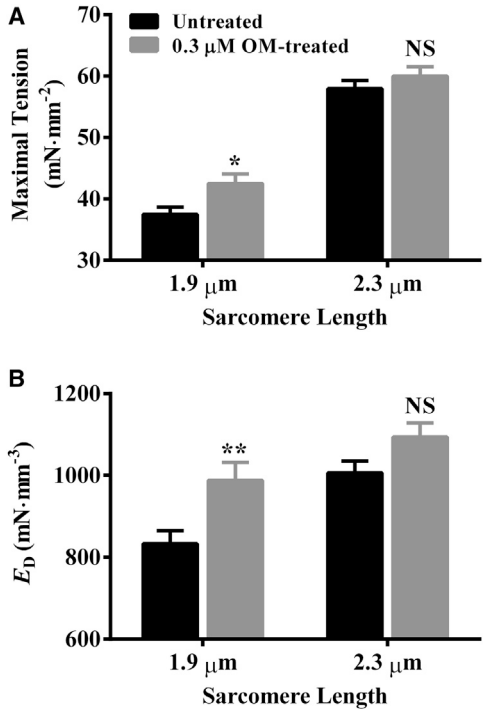

FIGURE 3 Effect of 0.3 μM OM on maximal tension and E_D. Steady-state tension was measured in muscle fibers at pCa 4.3, as described in the Supporting Material. E_D was estimated as the slope of the linear relationship between F_1 and F_{ss} (see Fig. 1) and the corresponding ML changes (ΔL). Bar graphs show the effect of 0.3 μM OM on (*A*) maximal tension and (*B*) E_D at short and long SL. Statistical differences were analyzed by two-way ANOVA and subsequent post hoc multiple pairwise comparisons using Fisher's least-squares difference method. Asterisks indicate a significant difference from untreated fibers (*$p < 0.05$, **$p < 0.01$; NS, not significant). A separate set of fibers from three hearts was used for each group. The numbers of fibers measured for untreated and 0.3-μM-OM-treated groups at short SL were 12 and 11, whereas those at long SL were 12 and 12, respectively. Data are expressed as the mean ± SE.

we used Hill model parameters, pCa_{50} (myofilament Ca^{2+} sensitivity), and n_H (myofilament cooperativity).

Two-way ANOVA of pCa_{50} showed a significant interaction effect ($p < 0.05$), suggesting that the effect of 0.3 μM OM on pCa_{50} varied in an SL-dependent manner. Post hoc analysis showed that the magnitude of increase in pCa_{50} was nearly twofold greater at short than at long SL in OM-treated fibers. When compared to the untreated group, 0.3 μM OM significantly increased pCa_{50} by 0.15 pCa units ($p < 0.001$; Fig. 4 *C*) at short SL, whereas it increased pCa_{50} by only 0.08 pCa units ($p < 0.001$; Fig. 4 *C*) at long SL; this suggested that LDA was altered. LDA was normal in untreated fibers because Ca^{2+} sensitivity increased significantly by 0.08 pCa units ($p < 0.001$; Fig. 4 *C*) when the SL was increased from 1.9 to 2.3 μm. In contrast, increasing the SL did not alter Ca^{2+} sensitivity significantly ($p = 0.33$; Fig. 4 *C*) in 0.3 μM OM-treated fibers, demonstrating that OM blunted LDA. A similar effect was also observed in 3.0-μM-OM-treated fibers (Table S1), demonstrating that LDA was blunted regardless of the OM concentration. As for n_H, two-way ANOVA did not show a significant interaction effect ($p = 0.56$), but it confirmed significant main effects of both OM ($p < 0.001$) and SL ($p < 0.001$). Treatment with 0.3 μM OM significantly decreased n_H in cardiac fibers by 22% ($p < 0.001$; Fig. 4 *D*) at short SL and by 32% ($p < 0.001$; Fig. 4 *D*) at long SL. An increase in SL significantly decreased n_H by 20% ($p < 0.001$; Fig. 4 *D*) in untreated fibers and by 30% ($p < 0.001$; Fig. 4 *D*) in 0.3-μM-OM-treated fibers. Although the SL dependency of n_H was not different between untreated and 0.3-μM-OM-treated fibers, OM attenuated n_H at both SLs, a finding that was also substantiated by our observations in the presence of 3.0 μM OM (Table S1).

Effect of OM on *c*

To determine whether OM altered XB detachment kinetics in an SL-dependent manner, we measured c at pCa 4.3. As demonstrated previously, c is an approximate measure of the XB detachment rate, g (24,25). A comparison of force responses to a sudden 2% stretch showed that OM induced a rightward shift in the force decay phase at both short (Fig. 5 *A*) and long SLs (Fig. 5 *B*), suggesting slower c; however, such OM-induced rightward shift in the force decay phase was more pronounced at short SL. This differential attenuation of c in 0.3-μM-OM-treated fibers at short and long SL gave rise to a significant interaction effect ($p < 0.01$). Treatment with 0.3 μM OM significantly decreased c by 40% ($p < 0.001$; Fig. 5 *C*) at short SL, whereas it decreased c by only 19% ($p < 0.05$; Fig. 5 *C*) at long SL. An increase in SL from 1.9 to 2.3 μm significantly attenuated c by 29% ($p < 0.001$; Fig. 5 *C*) in untreated fibers, whereas it did not show a significant effect on c ($p = 0.66$; Fig. 5 *C*) in 0.3-μM-OM-treated fibers. This observation demonstrated that OM abolished the SL dependency of c, which was supported by our data from 3.0-μM-OM-treated fibers (Table S1).

Effect of OM on k_{tr} and *b*

To determine whether OM altered the XB turnover rate in an SL-dependent manner, we measured k_{tr} and b at pCa 4.3. A comparison of force responses to the slack-restretch maneuver showed a rightward shift in the rising phase of 0.3-μM-OM-treated fibers at both SLs (Fig. 6, *A* and *B*), suggesting a slower k_{tr}. Our analysis of k_{tr} did not show a significant interaction effect ($p = 0.10$), but it showed significant main effects of both OM ($p < 0.001$) and SL ($p < 0.05$). Treatment with 0.3 μM OM significantly decreased k_{tr} by 61% ($p < 0.001$; Fig. 6 *C*) at short SL and by 57% ($p < 0.001$; Fig. 6 *C*) at long SL. An increase in SL from 1.9 to 2.3 μm significantly decreased k_{tr} by 0.40 s^{-1} ($p < 0.001$; Fig. 6 *C*) in untreated fibers, wheras it did not decrease k_{tr} significantly (0.08 s^{-1}; $p = 0.54$; Fig. 6 *C*) in 0.3 μM OM-treated fibers. This observation demonstrated that OM abolished the SL dependency of k_{tr}, a finding that was substantiated by our data from 3.0-μM-OM-treated fibers (Table S1).

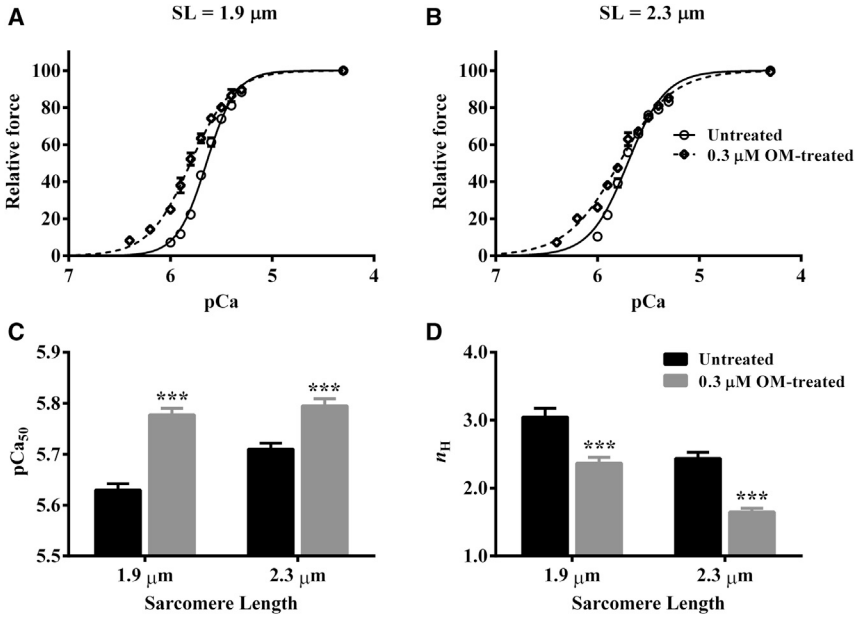

FIGURE 4 Effect of 0.3 μM OM on the pCa-tension relationship. pCa-tension relationships were measured using methods described in the Supporting Material. The Hill model was fitted to the pCa-tension relationships to derive pCa_{50} and n_H. (*A* and *B*) Effect of 0.3 μM OM on the pCa-tension relationship at (*A*) short SL and (*B*) long SL. (*C* and *D*) Bar graphs show the effect of 0.3 μM OM on (*C*) pCa_{50} and (*D*) n_H at short and long SL. Statistical differences were analyzed by two-way ANOVA and subsequent post hoc multiple pairwise comparisons using Fisher's least-squares difference method. Asterisks indicate a significant difference from untreated fibers (***$p < 0.001$). A separate set of fibers from three hearts was used for each group. The numbers of fibers measured for untreated and 0.3 μM OM groups at short SL were 12 and 11, whereas those at long SL were 12 and 12, respectively. Data are expressed as the mean ± SE.

The OM-mediated effect on XB recruitment dynamics was determined by estimating *b*. A comparison of force responses to a sudden 2% stretch indicated a slower rate of delayed force rise at both SLs (Fig. 5, *A* and *B*), suggesting slower *b*. Two-way ANOVA of *b* did not show a significant interaction effect ($p = 0.78$), but it confirmed significant main effects of both OM ($p < 0.001$) and SL ($p < 0.01$). Treatment with 0.3 μM OM significantly decreased *b* at both SLs by 22% ($p < 0.001$; Fig. 6 *D*) at short SL and 17% ($p < 0.001$; Fig. 6 *D*) at long SL, suggesting that the attenuating effect of OM on *b* was similar at both SLs. Consequently, the SL dependency of *b* was unaltered by OM, because an increase in SL significantly increased *b* by 10% ($p < 0.05$; Fig. 6 *D*) in untreated fibers and by 16% ($p < 0.05$; Fig. 6 *D*) in 0.3-μM-OM-treated fibers. Our observations on the attenuating effect of OM on *b* are corroborated by our observations in the presence of 3.0 μM OM (Table S1).

Effect of OM on E_R

To investigate whether OM altered the magnitude of stretch activation in an SL-dependent manner, we measured E_R at pCa 4.3. E_R is estimated from the new steady-state force (F_{nss}; Fig. 1 *B*) that results from a sudden increase in ML (Fig. 1 *A*), as described in the Supporting Material. Two-way ANOVA of E_R did not show a significant interaction effect ($p = 0.65$), but it confirmed significant main effects of both OM ($p < 0.001$) and SL ($p < 0.001$). Treatment with 0.3 μM OM significantly increased E_R by 36% ($p < 0.01$; Fig. 7) at short SL and 16% ($p < 0.05$; Fig. 7) at long SL, demonstrating that the OM-mediated increase in E_R was lower at long SL. Consequently, our data showed that the increase in E_R associated with an increase in SL from 1.9 to 2.3 μm (ΔE_R) is attenuated by OM. For example, ΔE_R was 82% ($p < 0.001$; Fig. 7) in untreated fibers, but this was only 54% ($p < 0.001$; Fig. 7) in 0.3-μM-OM-treated fibers. The attenuating effect of 0.3 μM OM on ΔE_R was substantiated by our data from 3.0-μM-OM-treated fibers (Table S1).

DISCUSSION

The impact of OM on the SL dependency of myofilament Ca^{2+} sensitivity has not been studied before. A major finding in our study is that the SL-dependent increase in myofilament Ca^{2+} sensitivity, ΔpCa_{50}, is abolished by OM. Our data also demonstrate that OM abolishes the SL dependency of *c* and k_{tr} at both concentrations (0.3 and 3.0 μM) of OM. We discuss the mechanisms by which OM-mediated effects on cardiac myofilaments are differently affected by changes in SL.

As others have observed before (5–8), pCa_{50} increases at long SL in OM-treated fibers (Fig. 4 *C*). A novel finding of our study, to our knowledge, is that OM increases pCa_{50} to a greater extent at short SL than at long SL (Fig. 4 *C*); a consequence of this effect at short SL is that an increase in SL does not increase pCa_{50} any further in OM-treated fibers. This observation suggests that mechanisms that underlie SL-mediated increase in pCa_{50} are saturated at short SL. Therefore, OM abolishes the ML-mediated increase in pCa_{50} (Fig. 4 *C*), which is known to be prominent in normal cardiac muscle fibers (9–11). To decompose mechanisms that are saturated at short SL, we must consider some fundamental aspects of LDA that are associated with the length-mediated increase in pCa_{50}. The basic prevailing view of LDA is that the steeper dependency of pCa_{50} on SL in

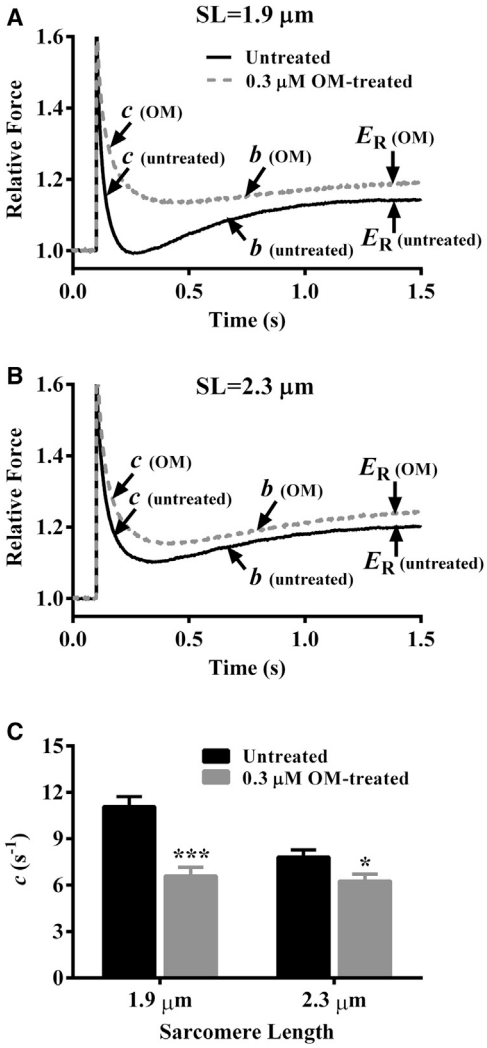

FIGURE 5 Effect of 0.3 μM OM on c. Effect of 0.3 μM OM on force responses to a 2% sudden stretch at (*A*) short SL and (*B*) long SL. Force data were normalized by the isometric steady-state value before ML perturbation. c describes the rate of force decay to a minimal force point, b represents the rate constant of delayed force rise, and E_R represents the ML-mediated increase in the steady-state force (24). Parameters b, c, and E_R are estimated by fitting the nonlinear recruitment-distortion model to a family of force responses to various-amplitude ML perturbations (24). (*C*) Bar graph showing the effect of 0.3 μM OM on c at short and long SL. Statistical differences were analyzed by two-way ANOVA and subsequent post hoc multiple pairwise comparisons using Fisher's least-squares difference method. Asterisks indicate a significant difference from untreated fibers ($*p < 0.05$, $***p < 0.001$). A separate set of fibers from three hearts was used for each group. The numbers of fibers measured for untreated and 0.3 μM OM groups at short SL were 12 and 11, whereas those at long SL were 12 and 12, respectively. Data are expressed as mean ± SE.

cardiac muscle results from the SL-mediated effects on thin-filament cooperativity. SL-mediated effects increase pCa_{50}, leading to the recruitment of new force-bearing XBs (9,12–15). Because OM-treated fibers deviate significantly from normal behavior, it suggests that mechanisms associated with LDA are altered in OM-treated fibers, especially at short SL.

Our contractile studies at short and long SL show several changes in contractile parameters that may help explain altered LDA in OM-treated fibers. Although there is a small but significant increase (13%) in tension at maximal activation at short SL, what is striking is the augmenting effect of OM on tension at submaximal activation. For instance, relative to untreated fibers, there is an ~160% increase in tension at half-maximal activation (pCa 5.8) in 0.3-μM-OM-treated fibers (Table S2), indicating that OM significantly increases the number of force-bearing XBs at submaximal activation. A consequence of such an increase in force-bearing XBs at submaximal activation is that it enhances XB-based activation of thin filaments via XB-XB and XB-regulatory unit (RU; troponin-tropomyosin) cooperative mechanisms; with respect to these two cooperative mechanisms, the consequences of augmented XB-RU cooperativity are of particular importance to our focus on pCa_{50}. It is generally known that XB-RU cooperativity is one of the important mechanisms that underpins the molecular basis for the length-mediated increase in pCa_{50} (14,28). An indirect effect of such an increase in XB-based effects is that it engages more RUs in XB-RU cooperativity, leaving behind fewer RUs in the recruitable pool. Therefore, RU-RU cooperativity is expected to decrease in OM-treated fibers; our data confirm this because a decrease in RU-RU cooperativity increases pCa_{50} (Fig. 4 *C*) and decreases n_H (Fig. 4 *D*; (14)). The combined effects of increased XB-based cooperativity and decreased RU-RU cooperativity (an indirect effect of OM on thin-filament activation) increases pCa_{50} substantially at short SL.

At long SL, pCa_{50} does not increase above that of short SL in OM-treated fibers. The saturation of increased XB-RU and decreased RU-RU cooperativity at short SL may provide the molecular basis for the lack of increase in pCa_{50} as SL increases. Due to the OM-mediated increase in the engagement of RUs in XB-RU cooperativity at short SL, there is limited capacity for the XB-RU population to rise as SL increases. The observation made at 0.3 μM OM was also valid for 3.0 μM, because pCa_{50} increased at short SL to such an extent that pCa_{50} did not increase any further at long SL (Table S1). We also observe a differential effect on the magnitude of E_R at short and long SL in OM-treated fibers; for example, OM increases E_R to a greater extent at short SL (36% at 1.9 μm and 16% at 2.3 μm). This effect is even more pronounced at submaximal activation (pCa 5.8); OM increases E_R by 58% at short SL, without any change at long SL (Table S2). Previous studies have shown that an increase in XB-based cooperativity augments E_R, whereas a decrease in XB-based cooperativity attenuates E_R (25,29,30). Collectively, these observations substantiate the idea that XB-based cooperativity is greater at short SL in OM-treated fibers.

OM-mediated increase in XB-based cooperativity may also affect other contractile parameters. Previous studies have shown that an increase in XB-based cooperativity

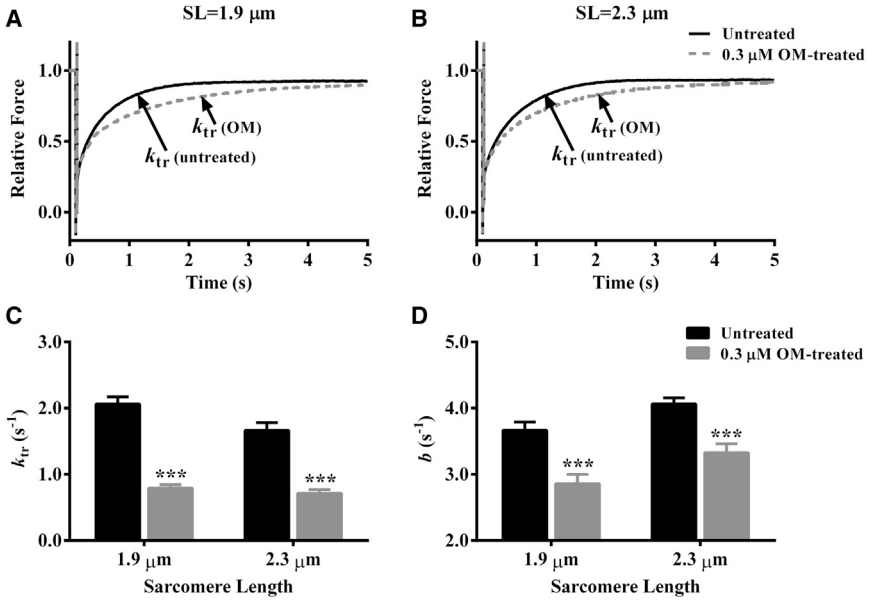

FIGURE 6 Effect of 0.3 μM OM on k_{tr} and b. k_{tr} describes the rate of tension redevelopment and is estimated by fitting a mono-exponential function to the rising phase of the force response to a large release-restretch length maneuver (38). b represents the rate constant of delayed force rise after a sudden stretch and is estimated by fitting the nonlinear recruitment-distortion model (24) to a family of force responses to various-amplitude length perturbations (see Figs. 1 and 5, *A* and *B*). (*A* and *B*) Effect of 0.3 μM OM on the force response to a large release-restretch maneuver at (*A*) short SL and (*B*) long SL. Force data were normalized by the isometric steady-state value before length perturbation. (*C* and *D*) Bar graph showing the effect of 0.3 μM OM on (*C*) k_{tr} and (*D*) b at short and long SL. Statistical differences were analyzed by two-way ANOVA and subsequent post hoc multiple pairwise comparisons using Fisher's least-squares difference method. Asterisks indicate a significant difference from untreated fibers (***$p < 0.001$). A separate set of fibers from three hearts was used for each group. The numbers of fibers measured for untreated and 0.3-μM-OM-treated groups at short SL were 12 and 11, whereas those at long SL were 12 and 12, respectively. Data are expressed as the mean ± SE.

slows k_{tr} (14,31) and OM attenuates k_{tr} at long SL (6,7). A new finding of our study, to our knowledge, shows that k_{tr} is also attenuated at short SL (Fig. 6 *C*). Therefore, significant attenuation of k_{tr} in OM-treated fibers at both short and long SL (Fig. 6 *C*) may be attributed to enhanced XB-based cooperativity. This is further substantiated by the observation that b is attenuated significantly at both short and long SL in OM-treated fibers (Fig. 6 *D*). Such observations regarding b are also valid at submaximal activation in 0.3-μM-OM-treated fibers (Table S2). Attenuation of k_{tr} in muscle fibers (5–7), including the finding from the study presented here, are in disagreement with previous in vitro studies (4,32,33), which have suggested that OM accelerates both the phosphate release and the transition of XBs from a weakly to a strongly bound state. Such discrepancy between muscle fiber studies and in vitro assays may result from the absence of lattice structure and poorly preserved cooperative mechanisms in in vitro assays. Despite some differences in observations, what is consistently observed is that OM increases the number of XBs at low levels of activation (5–8). The basis for the OM-mediated increase in the number of force-bearing XBs and the subsequent increase in XB-based cooperativity may be linked to the enhanced duty ratio of XBs, as suggested by previous studies (5–7), which is consistent with a significant decrease in g observed in our study. The increased duty ratio of XBs may promote recruitment of additional XBs via XB-based cooperative mechanisms (5,7).

The differential effects of OM on XB-based cooperativity at short and long SL has another interesting consequence for SL-mediated effects on XB cycling kinetics. Length-mediated effects on cardiac myofilaments have been shown to attenuate k_{tr} and g at long SL (34–36). Such changes are also evident in g (Fig. 5 *C*) and k_{tr} (Fig. 6 *C*) of untreated fibers in this study. What is interesting is that such an SL-mediated attenuating effect on k_{tr} is abolished in OM-treated fibers. Attenuation of k_{tr} at short SL may be attributed to enhanced XB-based cooperativity (31). This attenuating effect on k_{tr} appears to be saturated at short SL, because there is no further attenuation at long SL (Fig. 6 *C*). Attenuation

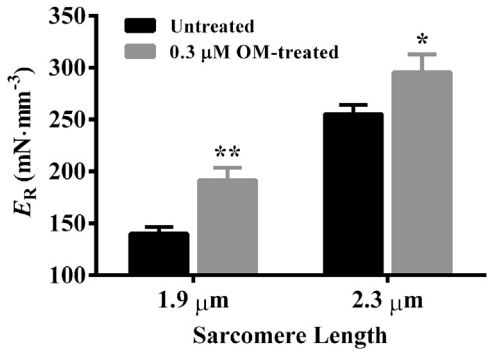

FIGURE 7 Effect of 0.3 μM OM on E_R. E_R is the magnitude of stretch activation and is estimated as the slope of the linear relationship between (F_{nss}-F_{ss}) and imposed ML changes, ΔL (also see Figs. 1 and 5, *A* and *B*). Statistical differences were analyzed by two-way ANOVA and subsequent post-hoc multiple pairwise comparisons using Fisher's least-squares difference method. Asterisks indicate significantly different from untreated fibers (*$p < 0.05$, **$p < 0.01$). A separate set of fibers from three hearts was used for each group. The number of fibers measured for untreated and 0.3 μM OM groups at short SL were 12 and 11, while those at long SL were 12 and 12, respectively. Data are expressed as mean ± SE.

of k_{tr} in OM-treated fibers may be explained by a decrease in g (34,37–39).

Two plausible mechanisms have been suggested to explain how OM decreases g (7): 1) OM may decrease g by slowing the rate of ADP release, although direct evidence is lacking; and 2) OM may decrease g by slowing the isomerization step between strongly bound actomyosin-ADP states that precedes the XB detachment step. The new finding from this study, to our knowledge, shows that g is also attenuated at short SL, but the magnitude of attenuation is greater at short SL; for example, g is attenuated by 40% at short SL and by 20% at long SL in 0.3-μM-OM-treated fibers (Fig. 5 *C*). Such observations regarding g are also valid at submaximal activations in 0.3-μM-OM-treated fibers (Table S2). A consequence of this greater attenuation of g at short SL is that the SL dependency of g is ablated (Fig. 5 *C*) in a manner similar to that observed for k_{tr} (Fig. 6 *C*). These observations are also supported by data from fibers treated with 3.0 μM OM (Table S1). Collectively, the observations made above substantiate the notion that OM alters mechanisms linked to LDA.

Relevance of our findings to whole heart function

Previous studies in both animal models (2,4) and humans (1,3) suggest that OM enhances systolic function by prolonging the systolic ejection time. Changes in b and E_R shed some light on how OM may tune the late phase of ejection. The slower b in OM-treated fibers suggests a slower rise in XB recruitment, which prolongs the effect of stretch activation on ventricular force output (39–42). Augmentation of E_R suggests an increase in ventricular force output during the late phase of ejection. Such enhanced force output during the late stage of systole—paired with the increased Ca^{2+} sensitivity and lengthened duty ratio of XBs (due to slower g)—may significantly increase stroke volume by prolonging the duration of systole. Although these changes suggest improved systolic function, they may adversely affect diastole not only by delaying the onset of ventricular relaxation but also by slowing isovolumic relaxation. Such OM-mediated effects on relaxation may reduce the amount of venous filling in the next beat, a possibility that requires further investigation.

New observations from our study demonstrate that OM has a major effect on Ca^{2+} sensitivity and LDA, leading us to speculate that it may modify the FS mechanism to some extent in the intact heart. Indeed, changes in myofilament Ca^{2+} sensitivity have been shown to impair FS mechanism in intact hearts (16–19). OM-mediated blunting of LDA may attenuate the ability of the heart to increase stroke volume in response to an increase in venous return during exertion. This may have some relevance to a recent clinical study in which OM-treated patients with systolic dysfunction exhibited a decreasing trend in exercise time by 30%, although authors noted that this decrease did not reach statistical significance due to the smaller sample size (43). Thus, new findings from our contractile study, along with the observations from the aforementioned study, warrant further investigation regarding the effect of OM on the FS mechanism at the whole-heart level.

SUPPORTING MATERIAL

Supporting Materials and Methods, one figure, and two tables are available at http://www.biophysj.org/biophysj/supplemental/S0006-3495(17)30752-X.

AUTHOR CONTRIBUTIONS

Study conception and design, data acquisition, data analysis and interpretation, and drafting of the manuscript, S.K.G.; Data acquisition, data analysis and interpretation, and drafting of the manuscript, S.M.R.; Study conception and design, data interpretation, and drafting of the manuscript, M.C.

SUPPORTING CITATIONS

References (44–51) appear in the Supporting Material.

REFERENCES

1. Cleland, J. G., J. R. Teerlink, …, F. I. Malik. 2011. The effects of the cardiac myosin activator, omecamtiv mecarbil, on cardiac function in systolic heart failure: a double-blind, placebo-controlled, crossover, dose-ranging phase 2 trial. *Lancet.* 378:676–683.
2. Shen, Y. T., F. I. Malik, …, S. F. Vatner. 2010. Improvement of cardiac function by a cardiac Myosin activator in conscious dogs with systolic heart failure. *Circ Heart Fail.* 3:522–527.
3. Teerlink, J. R., C. P. Clarke, …, A. A. Wolff. 2011. Dose-dependent augmentation of cardiac systolic function with the selective cardiac myosin activator, omecamtiv mecarbil: a first-in-man study. *Lancet.* 378:667–675.
4. Malik, F. I., J. J. Hartman, …, D. J. Morgans. 2011. Cardiac myosin activation: a potential therapeutic approach for systolic heart failure. *Science.* 331:1439–1443.
5. Mamidi, R., K. S. Gresham, …, J. E. Stelzer. 2015. Molecular effects of the myosin activator omecamtiv mecarbil on contractile properties of skinned myocardium lacking cardiac myosin binding protein-C. *J. Mol. Cell. Cardiol.* 85:262–272.
6. Nagy, L., Á. Kovács, …, Z. Papp. 2015. The novel cardiac myosin activator omecamtiv mecarbil increases the calcium sensitivity of force production in isolated cardiomyocytes and skeletal muscle fibres of the rat. *Br. J. Pharmacol.* 172:4506–4518.
7. Swenson, A. M., W. Tang, …, C. M. Yengo. 2017. Omecamtiv mecarbil enhances the duty ratio of human β-cardiac myosin resulting in increased calcium sensitivity and slowed force development in cardiac muscle. *J. Biol. Chem.* 292:3768–3778.
8. Utter, M. S., D. M. Ryba, …, R. J. Solaro. 2015. Omecamtiv mecarbil, a cardiac myosin activator, increases Ca^{2+} sensitivity in myofilaments with a dilated cardiomyopathy mutant tropomyosin E54K. *J. Cardiovasc. Pharmacol.* 66:347–353.
9. Allen, D. G., and J. C. Kentish. 1985. The cellular basis of the length-tension relation in cardiac muscle. *J. Mol. Cell. Cardiol.* 17:821–840.
10. Konhilas, J. P., T. C. Irving, and P. P. de Tombe. 2002. Length-dependent activation in three striated muscle types of the rat. *J. Physiol.* 544:225–236.
11. Wang, Y. P., and F. Fuchs. 1994. Length, force, and Ca^{2+}-troponin C affinity in cardiac and slow skeletal muscle. *Am. J. Physiol.* 266: C1077–C1082.

12. Fitzsimons, D. P., and R. L. Moss. 1998. Strong binding of myosin modulates length-dependent Ca^{2+} activation of rat ventricular myocytes. *Circ. Res.* 83:602–607.
13. Moss, R. L., and D. P. Fitzsimons. 2002. Frank-Starling relationship: long on importance, short on mechanism. *Circ. Res.* 90:11–13.
14. Razumova, M. V., A. E. Bukatina, and K. B. Campbell. 2000. Different myofilament nearest-neighbor interactions have distinctive effects on contractile behavior. *Biophys. J.* 78:3120–3137.
15. Smith, L., C. Tainter, …, D. A. Martyn. 2009. Cooperative cross-bridge activation of thin filaments contributes to the Frank-Starling mechanism in cardiac muscle. *Biophys. J.* 96:3692–3702.
16. Abraham, D. M., R. T. Davis, 3rd, …, H. A. Rockman. 2016. β-Arrestin mediates the Frank-Starling mechanism of cardiac contractility. *Proc. Natl. Acad. Sci. USA.* 113:14426–14431.
17. Arteaga, G. M., K. A. Palmiter, …, R. J. Solaro. 2000. Attenuation of length dependence of calcium activation in myofilaments of transgenic mouse hearts expressing slow skeletal troponin I. *J. Physiol.* 526: 541–549.
18. Layland, J., D. J. Grieve, …, A. M. Shah. 2004. Essential role of troponin I in the positive inotropic response to isoprenaline in mouse hearts contracting auxotonically. *J. Physiol.* 556:835–847.
19. Nowak, G., J. R. Peña, …, B. M. Wolska. 2007. Correlations between alterations in length-dependent Ca^{2+} activation of cardiac myofilaments and the end-systolic pressure-volume relation. *J. Muscle Res. Cell Motil.* 28:415–419.
20. Ford, S. J., R. Mamidi, …, M. Chandra. 2012. Effects of R92 mutations in mouse cardiac troponin T are influenced by changes in myosin heavy chain isoform. *J. Mol. Cell. Cardiol.* 53:542–551.
21. Sequeira, V., P. J. Wijnker, …, J. van der Velden. 2013. Perturbed length-dependent activation in human hypertrophic cardiomyopathy with missense sarcomeric gene mutations. *Circ. Res.* 112:1491–1505.
22. van Dijk, S. J., E. R. Paalberends, …, J. van der Velden. 2012. Contractile dysfunction irrespective of the mutant protein in human hypertrophic cardiomyopathy with normal systolic function. *Circ Heart Fail.* 5:36–46.
23. Schwinger, R. H., M. Böhm, …, E. Erdmann. 1994. The failing human heart is unable to use the Frank-Starling mechanism. *Circ. Res.* 74: 959–969.
24. Ford, S. J., M. Chandra, …, K. B. Campbell. 2010. Model representation of the nonlinear step response in cardiac muscle. *J. Gen. Physiol.* 136:159–177.
25. Campbell, K. B., M. Chandra, …, W. C. Hunter. 2004. Interpreting cardiac muscle force-length dynamics using a novel functional model. *Am. J. Physiol. Heart Circ. Physiol.* 286:H1535–H1545.
26. Chandra, V., S. K. Gollapudi, and M. Chandra. 2015. Rat cardiac troponin T mutation (F72L)-mediated impact on thin filament cooperativity is divergently modulated by α- and β-myosin heavy chain isoforms. *Am. J. Physiol. Heart Circ. Physiol.* 309:H1260–H1270.
27. Reda, S. M., S. K. Gollapudi, and M. Chandra. 2016. L71F mutation in rat cardiac troponin T augments crossbridge recruitment and detachment dynamics against α-myosin heavy chain, but not against β-myosin heavy chain. *J. Muscle Res. Cell Motil.* 37:215–223.
28. de Tombe, P. P., R. D. Mateja, …, T. C. Irving. 2010. Myofilament length dependent activation. *J. Mol. Cell. Cardiol.* 48:851–858.
29. Campbell, K. B., and M. Chandra. 2006. Functions of stretch activation in heart muscle. *J. Gen. Physiol.* 127:89–94.
30. Stelzer, J. E., L. Larsson, …, R. L. Moss. 2006. Activation dependence of stretch activation in mouse skinned myocardium: implications for ventricular function. *J. Gen. Physiol.* 127:95–107.
31. Campbell, K. 1997. Rate constant of muscle force redevelopment reflects cooperative activation as well as cross-bridge kinetics. *Biophys. J.* 72:254–262.
32. Liu, Y., H. D. White, …, E. Forgacs. 2015. Omecamtiv mecarbil modulates the kinetic and motile properties of porcine β-cardiac myosin. *Biochemistry.* 54:1963–1975.
33. Winkelmann, D. A., E. Forgacs, …, A. M. Stock. 2015. Structural basis for drug-induced allosteric changes to human β-cardiac myosin motor activity. *Nat. Commun.* 6:7974.
34. Chandra, M., M. L. Tschirgi, …, K. B. Campbell. 2006. Troponin T modulates sarcomere length-dependent recruitment of cross-bridges in cardiac muscle. *Biophys. J.* 90:2867–2876.
35. Ford, S. J., and M. Chandra. 2013. Length-dependent effects on cardiac contractile dynamics are different in cardiac muscle containing α- or β-myosin heavy chain. *Arch. Biochem. Biophys.* 535:3–13.
36. Korte, F. S., and K. S. McDonald. 2007. Sarcomere length dependence of rat skinned cardiac myocyte mechanical properties: dependence on myosin heavy chain. *J. Physiol.* 581:725–739.
37. Adhikari, B. B., M. Regnier, …, D. A. Martyn. 2004. Cardiac length dependence of force and force redevelopment kinetics with altered cross-bridge cycling. *Biophys. J.* 87:1784–1794.
38. Brenner, B., and E. Eisenberg. 1986. Rate of force generation in muscle: correlation with actomyosin ATPase activity in solution. *Proc. Natl. Acad. Sci. USA.* 83:3542–3546.
39. Stelzer, J. E., and R. L. Moss. 2006. Contributions of stretch activation to length-dependent contraction in murine myocardium. *J. Gen. Physiol.* 128:461–471.
40. Davis, J. S., S. Hassanzadeh, …, N. D. Epstein. 2001. The overall pattern of cardiac contraction depends on a spatial gradient of myosin regulatory light chain phosphorylation. *Cell.* 107:631–641.
41. Stelzer, J. E., D. P. Fitzsimons, and R. L. Moss. 2006. Ablation of myosin-binding protein-C accelerates force development in mouse myocardium. *Biophys. J.* 90:4119–4127.
42. Stelzer, J. E., J. R. Patel, and R. L. Moss. 2006. Protein kinase A-mediated acceleration of the stretch activation response in murine skinned myocardium is eliminated by ablation of cMyBP-C. *Circ. Res.* 99:884–890.
43. Greenberg, B. H., W. Chou, …, T. Shaburishvili. 2015. Safety and tolerability of omecamtiv mecarbil during exercise in patients with ischemic cardiomyopathy and angina. *JACC Heart Fail.* 3:22–29.
44. Chandra, M., M. L. Tschirgi, …, K. B. Campbell. 2007. Interaction between myosin heavy chain and troponin isoforms modulate cardiac myofiber contractile dynamics. *Am. J. Physiol. Regul. Integr. Comp. Physiol.* 293:R1595–R1607.
45. de Tombe, P. P., and G. J. Stienen. 1995. Protein kinase A does not alter economy of force maintenance in skinned rat cardiac trabeculae. *Circ. Res.* 76:734–741.
46. Fabiato, A., and F. Fabiato. 1979. Calculator programs for computing the composition of the solutions containing multiple metals and ligands used for experiments in skinned muscle cells. *J. Physiol. (Paris).* 75:463–505.
47. Gollapudi, S. K., C. E. Gallon, and M. Chandra. 2013. The tropomyosin binding region of cardiac troponin T modulates crossbridge recruitment dynamics in rat cardiac muscle fibers. *J. Mol. Biol.* 425: 1565–1581.
48. Gollapudi, S. K., R. Mamidi, …, M. Chandra. 2012. The N-terminal extension of cardiac troponin T stabilizes the blocked state of cardiac thin filament. *Biophys. J.* 103:940–948.
49. Gollapudi, S. K., J. C. Tardiff, and M. Chandra. 2015. The functional effect of dilated cardiomyopathy mutation (R144W) in mouse cardiac troponin T is differently affected by α- and β-myosin heavy chain isoforms. *Am. J. Physiol. Heart Circ. Physiol.* 308:H884–H893.
50. Mamidi, R., and M. Chandra. 2013. Divergent effects of α- and β-myosin heavy chain isoforms on the N terminus of rat cardiac troponin T. *J. Gen. Physiol.* 142:413–423.
51. Stienen, G. J., R. Zaremba, and G. Elzinga. 1995. ATP utilization for calcium uptake and force production in skinned muscle fibres of *Xenopus laevis*. *J. Physiol.* 482:109–122.

Biophysical Journal, Volume *113*

Supplemental Information

Omecamtiv Mecarbil Abolishes Length-Mediated Increase in Guinea Pig Cardiac Myofiber Ca^{2+} Sensitivity

Sampath K. Gollapudi, Sherif M. Reda, and Murali Chandra

MATERIALS AND METHODS

Determination of phosphorylation status of sarcomeric proteins in untreated and OM-treated fibers: Untreated and 0.3 μM OM-treated left ventricular papillary muscle fibers were solubilized using a muscle protein extraction buffer (2.5% SDS, 10% glycerol, 50 mM tris base (pH 6.8 at 4ºC), 1 mM Dithiothreitol, 4 mM benzamidine HCl, and a cocktail of phosphatase/protease inhibitors). The final concentrations of all samples were adjusted to 2 mg/ml using protein loading dye (125 mM Tris-HCl (pH 6.8), 20% glycerol, 2% SDS, 0.01% bromophenol blue, and 50 mM β-mercaptoethanol). Equal quantities (10 μg) of standardized protein samples were loaded and ran on a 12.5% small SDS gel. The gel was fixed in a solution containing 50% methanol and 10% acetic acid, and then treated with Pro-Q diamond stain and destain (P33300 and P33310, Life Technologies, Grand Island, NY), as described in the Life Technologies manual. Phosphoproteins were visualized by imaging the gel using UV transillumination on a BioRad ChemiDoc XRS camera.

Preparation of detergent-skinned cardiac muscle fibers: Left ventricular papillary muscle fibers from guinea pigs were prepared using methods described previously (1-3). Briefly, guinea pigs were deeply anesthetized using isoflurane, and hearts were quickly excised and placed into an ice-cold high-relaxing (HR) solution containing the following (in mM): 20 2,3-butanedione monoxime (BDM), 50 *N*,*N*-bis (2-hydroxyethyl)-2-amino-ethane-sulfonic acid (BES), 30.83 potassium propionate (K-prop), 10 sodium azide (NaN_3), 20 ethylene glycol tetra-acetic acid (EGTA), 6.29 magnesium chloride ($MgCl_2$), 6.09 Na_2ATP, 4.0 benzamidine HCl, 1.0 of dithiothreitol (DTT), and a cocktail of protease inhibitors. Left ventricular papillary muscle bundles were quickly removed in HR solution, dissected into smaller sections measuring 2.0–2.5

mm in length and 150–200 μm in thickness, and were detergent-skinned overnight in HR solution containing 1% Triton-X-100.

Measurements of pCa-tension relationship: Steady-state isometric tension measurements in muscle fibers were made at various pCa ($-\log_{10}$ of $[Ca^{2+}]_{free}$), as described before (2,4-6). In brief, muscle fibers were attached between a motor arm (322C, Aurora Scientific Inc., Ontario, Canada) and a force transducer (AE 801, Sensor One Technologies, Sausalito, CA) using T-shaped aluminum clips. The sarcomere length (SL) of muscle fibers was adjusted to either 1.9 or 2.3 μm in HR solution using He-Ne laser diffraction technique (5). Following two cycles of maximal activation (pCa 4.3) and relaxation (pCa 9.0), SL was readjusted to the desired SL if necessary. The muscle length (ML) and cross-sectional area (CSA) were measured and then muscle fibers were exposed to various solutions with pCa ranging from 4.3 to 9.0 in a constantly-stirred chamber. Force responses were recorded on a computer at a sampling rate of 1 kHz. Isometric steady-state tension values were plotted against pCa to construct the pCa-tension relationship. The Hill equation was fitted to the normalized pCa-tension relationship to estimate two parameters, n_H (myofilament cooperativity) and pCa_{50} (myofilament Ca^{2+} sensitivity). All measurements are made at 20ºC.

pCa solutions and their compositions: Compositions of pCa 9.0 and pCa 4.3 solutions were calculated based on the program by Fabiato and Fabiato (7). pCa 9.0 solution contained the following (in mM): 50 BES, 5 NaN_3, 10 phosphoenol pyruvate (PEP), 10 EGTA, 0.024 calcium chloride ($CaCl_2$), 6.87 $MgCl_2$, 5.83 Na_2ATP, and 51.14 K-Prop, while pCa 4.3 solution contained the following (in mM): 50 BES, 5 NaN_3, 10 PEP, 10 EGTA, 10.11 $CaCl_2$, 6.61 $MgCl_2$, 5.95

Na_2ATP, and 31 K-Prop. Both pCa 9.0 and pCa 4.3 solutions included a cocktail of protease inhibitors ((in μM): 10 leupeptin, 1000 pepstatin, 100 PMSF, 20 diadenosine penta-phosphate, 10 oligomycin). The pH and ionic strength of pCa solutions were adjusted to 7.0 and 180 mM, respectively. All other intermediate pCa solutions were made by mixing appropriate amounts of pCa 9.0 and pCa 4.3 solutions, which were based on the program by Fabiato and Fabiato (7).

Dynamic muscle fiber stiffness: A series of various amplitude stretch/release perturbations (±0.5%, ±1.0%, ±1.5%, and ±2.0% of the initial ML) was applied on muscle fibers and the corresponding force responses were recorded (8). A non-linear recruitment-distortion (NLRD) model was fit to force responses, as described previously (8), to estimate four model parameters: the magnitude of the instantaneous muscle fiber stiffness caused by a sudden change in ML (E_D); the rate by which the strain within bound XBs dissipates to a steady-state level (c); the rate by which new XBs are recruited into the force-bearing state due to a change in ML (b); and the magnitude of increase in the muscle fiber stifness due to ML-mediated recruitment of additional force-bearing XBs (E_R). Below, we explain the physiological significance of various model parameters using 2% sudden stretch (Fig. 1 *A* in the main article) and the elicited force response (Fig. 1 *B*) from an untreated guinea pig cardiac muscle fiber.

***E*$_D$**: In phase 1, a sudden increase in ML (Fig. 1 *A*) causes an instantaneous increase in force from the isometric steady state value (F_{ss}) to F_1 (Fig. 1 *B*). F_1 results from the distortion of elastic elements within strongly-bound XBs. Thus, F_1 increases when the number of strong XBs in the steady state (prior to ML change) is higher and vice versa. Because E_D is estimated as the slope of the linear relationship between changes in F_1-F_{ss} and the imposed changes in ML (ΔL), it is an approximate measure of the number of strongly-bound XBs (8,9).

***c*:** In phase 2, when the muscle fiber is held at the increased ML (Fig. 1 *A*), force decays exponentially at a characteristic rate, *c* (Fig. 1 *B*). This rapid decay results from the detachment of distorted XBs, followed by their equilibration into the non-force bearing state. We have previously demonstrated that *c* is an approximate measure of XB detachment rate, *g* (9).

***b*:** In phase 3, force begins to rise gradually in an exponential fashion at a characteristic rate, *b* (Fig. 1 *B*). This gradual rise in force results from the recruitment of additional XBs into the force-bearing state.

***E*$_R$:** The steady rise in force during phase 3 levels off to a new steady-state value (F_{nss}) that is higher than F_{ss} (Fig. 1 *B*). The magnitude of increase, from F_{ss} to F_{nss}, is proportional to the number of additional force-bearing XBs recruited for a given increase in ML. Because E_R is derived as the slope of the linear relationship between changes in F_{nss}-F_{ss} and ΔL, it is an approximate measure of the magnitude of ML-mediated XB recruitment.

Rate constant of tension redevelopment (k_{tr}): k_{tr} was estimated using a modified version of the large slack/restretch maneuver originally described by Brenner and Eisenberg (10). The modified version is described in our earlier published works (11-13). Briefly, fully activated muscle fiber was rapidly slackened by 10% of the initial ML using a servo motor and was held for 25 ms at the reduced length. The muscle fiber was then rapidly (0.5 ms) stretched past the initial ML by 10%, brought back to the initial ML and allowed to redevelop force. k_{tr} was estimated by fitting the following mono-exponential function to the rising phase of the resulting force response:

$$F = (F_{ss} - F_{res})(1 - e^{-k_{tr}t}) + F_{res}$$

where F_{ss} is the steady-state isometric force and F_{res} is the residual force from which the fiber starts to redevelop force.

SUPPORTING REFERENCES

1. Ford, S. J., R. Mamidi, J. Jimenez, J. C. Tardiff, and M. Chandra. 2012. Effects of R92 mutations in mouse cardiac troponin T are influenced by changes in myosin heavy chain isoform. *J Mol Cell Cardiol* 53:542-551.

2. Gollapudi, S. K., J. C. Tardiff, and M. Chandra. 2015. The functional effect of dilated cardiomyopathy mutation (R144W) in mouse cardiac troponin T is differently affected by alpha- and beta-myosin heavy chain isoforms. *Am J Physiol Heart Circ Physiol* 308:H884-893.

3. Mamidi, R. and M. Chandra. 2013. Divergent effects of alpha- and beta-myosin heavy chain isoforms on the N terminus of rat cardiac troponin T. *J Gen Physiol* 142:413-423.

4. Chandra, M., M. L. Tschirgi, S. J. Ford, B. K. Slinker, and K. B. Campbell. 2007. Interaction between myosin heavy chain and troponin isoforms modulate cardiac myofiber contractile dynamics. *Am J Physiol Regul Integr Comp Physiol* 293:R1595-1607.

5. de Tombe, P. P. and G. J. Stienen. 1995. Protein kinase A does not alter economy of force maintenance in skinned rat cardiac trabeculae. *Circ Res* 76:734-741.

6. Stienen, G. J., R. Zaremba, and G. Elzinga. 1995. ATP utilization for calcium uptake and force production in skinned muscle fibres of Xenopus laevis. *J Physiol* 482 (Pt 1):109-122.

7. Fabiato, A. and F. Fabiato. 1979. Calculator programs for computing the composition of the solutions containing multiple metals and ligands used for experiments in skinned muscle cells. *J Physiol (Paris)* 75:463-505.

8. Ford, S. J., M. Chandra, R. Mamidi, W. Dong, and K. B. Campbell. 2010. Model representation of the nonlinear step response in cardiac muscle. *J Gen Physiol* 136:159-177.

9. Campbell, K. B., M. Chandra, R. D. Kirkpatrick, B. K. Slinker, and W. C. Hunter. 2004. Interpreting cardiac muscle force-length dynamics using a novel functional model. *Am J Physiol Heart Circ Physiol* 286:H1535-1545.

10. Brenner, B. and E. Eisenberg. 1986. Rate of force generation in muscle: correlation with actomyosin ATPase activity in solution. *Proc Natl Acad Sci USA* 83:3542-3546.

11. Ford, S. J. and M. Chandra. 2013. Length-dependent effects on cardiac contractile dynamics are different in cardiac muscle containing alpha- or beta-myosin heavy chain. *Arch Biochem Biophys* 535:3-13.

12. Gollapudi, S. K., C. E. Gallon, and M. Chandra. 2013. The tropomyosin binding region of cardiac troponin T modulates crossbridge recruitment dynamics in rat cardiac muscle fibers. *J Mol Biol* 425:1565-1581.

13. Gollapudi, S. K., R. Mamidi, S. L. Mallampalli, and M. Chandra. 2012. The N-terminal extension of cardiac troponin T stabilizes the blocked state of cardiac thin filament. *Biophys J* 103:940-948.

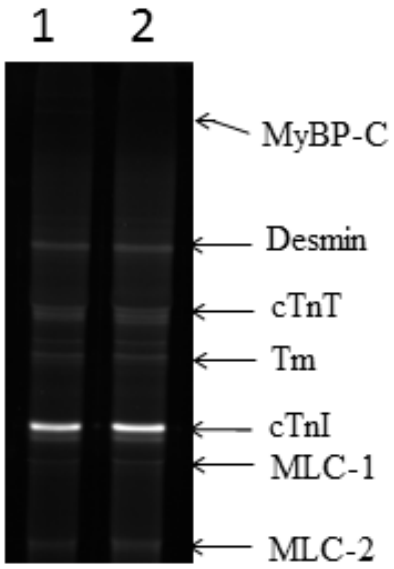

Figure S1 Pro-Q Diamond-stained gel showing the levels of phosphorylated proteins in untreated and 0.3 µM OM-treated fibers. Fibers were solubilized in 2.5% SDS solution and ran on a 12.5% SDS-gel. The gel was fixed in a solution containing 50% methanol and 10% acetic acid and then treated with Pro-Q diamond stain and destain, as described in Materials and Methods. A visual examination of the Pro-Q stained gel shows that the phosphorylation levels of various proteins are similar in untreated (*lane* 1) and OM-treated fibers (*lane* 2). MyBP-C, myosin binding protein-C; cTnT, cardiac troponin T; Tm, tropomyosin; cTnI, cardiac troponin I; MLC-1, myosin light chain 1; MLC-2, myosin light chain 2.

Table S1. Effects of 3.0 μM OM on SL-dependency of various contractile parameters.

Parameter	Untreated fibers			OM (3.0 μM)-treated fibers		
	1.9 μm	**2.3 μm**	**Δ**	**1.9 μm**	**2.3 μm**	**Δ**
Tension ($mN \cdot mm^{-2}$)	37.5±1.2	57.9±1.3	$+20.5^{***}$	42.1±0.72	55.6±1.1	$+13.5^{***}$
E_D ($mN \cdot mm^{-3}$)	813±27	1006±29	$+193^{***}$	955±26	1109±36	$+154^{**}$
pCa_{50}	5.63±0.01	5.71±0.01	$+0.08^{***}$	6.18±0.01	6.19±0.02	$+0.01^{NS}$
n_H	3.05±0.09	2.44±0.09	-0.61^{***}	1.09±0.05	0.96±0.06	-0.13^{NS}
c (s^{-1})	11.1±0.6	7.8±0.5	-3.30^{***}	2.45±0.27	1.75±0.20	-0.70^{NS}
b (s^{-1})	3.67±0.12	4.02±0.10	$+0.35^{NS}$	1.34±0.12	1.06±0.13	-0.28^{NS}
k_{tr} (s^{-1})	2.06±0.11	1.66±0.12	-0.40^{***}	0.28±0.01	0.26±0.01	-0.02^{NS}
E_R ($mN \cdot mm^{-3}$)	140±6	255±9	$+115^{***}$	141±7	225±11	$+84^{***}$

'Δ' represents the change in contractile parameter in response to an increase in SL from 1.9 to 2.3 μm ('+' indicates increase and '-' indicates decrease). Statistical differences were analyzed by two-way ANOVA and subsequent post-hoc Fisher's LSD method. Asterisks indicate significant difference when compared to the data at 1.9 μm (*P<0.05; **P<0.01; ***P<0.001; NS, not significant). A separate set of fibers from three hearts was used for each group. The number of fibers measured for untreated and 3.0 μM OM groups at short SL were 12 and 11, while those at long SL were 12 and 11, respectively. Data are expressed as Mean±SEM.

Table S2. Effects of 0.3 μM OM on SL-dependency of various contractile parameters at submaximal activation (pCa 5.8).

Parameter	Untreated fibers			OM (0.3 μM)-treated fibers		
	1.9 μm	**2.3 μm**	**Δ**	**1.9 μm**	**2.3 μm**	**Δ**
Tension ($mN \cdot mm^{-2}$)	8.3±0.7	22.9±1.8	$+14.6^{***}$	21.5±1.5	29.0±1.7	$+7.5^{***}$
E_D ($mN \cdot mm^{-3}$)	299±39	488±28	$+189^{***}$	540±27	676±35	$+136^{**}$
c (s^{-1})	11.1±0.8	8.1±0.5	-3.0^{**}	5.7±0.6	6.0±0.7	$+0.3^{NS}$
b (s^{-1})	2.0±0.2	2.1±0.1	$+0.1^{NS}$	1.4±0.1	1.6±0.1	$+0.2^{NS}$
E_R ($mN \cdot mm^{-3}$)	106±15	205±10	$+115^{***}$	172±13	206±17	$+34^{NS}$

'Δ' represents the change in contractile parameter in response to an increase in SL from 1.9 to 2.3 μm ('+' indicates increase and '-' indicates decrease). Statistical differences were analyzed by two-way ANOVA and subsequent post-hoc Fisher's LSD method. Asterisks indicate significant difference when compared to the data at 1.9 μm (**P<0.01; ***P<0.001; NS, not significant). A separate set of fibers from three hearts was used for each group. The number of fibers measured for untreated and 0.3 μM OM groups at short SL were 10 and 9, while those at long SL were 10 and 11, respectively. Data are expressed as Mean±SEM.